PS/LIN/Note 77-14
25 July 1977

EDGE EFFECT IN BEAM MONITORS

J.H. Cupérus
CERN, 1211 Genève 23

ABSTRACT

Quite often, particle-beam monitors have not the same cross-section as the beam pipe or vacuum chamber in which they are mounted. In that case, the electromagnetic field of the beam is distorted in the vicinity of the edges of the monitor. We compute this field, at the junction of two rectangular beam pipes of different dimensions, for a beam with constant charge along its length. Solutions which are less accurate but easier to apply are obtained with a first order approximation. The results are extended to intensity-modulated beams and circular or elliptical cross-sections. We compute the errors, due to the edge effect, for the electrostatic pickup and the wall-current monitor. The final formulas are simple and easy to apply to practical cases.

To be published in Nuclear Instruments and Methods.

1. INTRODUCTION

The electromagnetic field of a charged particle beam, in a cylindrical beam pipe with uniform cross-section, is well defined. If a beam monitor is mounted in such a beam pipe, without disturbing the profile of the pipe wall significantly, its response to the beam can usually be calculated with precision. Many practical beam monitors, however, do not conform to this ideal situation. An electrostatic pickup (ESPU), for instance, is often made slightly larger than the beam pipe, in order to protect it from the charge of stray particles (fig. 1). The reverse is true when the ESPU is mounted in a larger vacuum tank (fig. 2). An extreme case is an ESPU mounted on a beam in free air or around a glass or ceramic vacuum pipe. Discontinuities also occur when a wall-current monitor, with circular cross-section is joined, on both sides, to an elliptical beam pipe (fig. 3).

In all these cases, the field is distorted near the transitions in cross-section, in a not very well controlled way. To prevent errors in the measurement of the intensity or position of the beam, the immediate vicinity of the transition is not used for the measurement. For the ESPU, grounded guard rings are used and for the wall-current monitor, the gap can not be too close to a transition. Quite often, however, the longitudinal space is limited and the question is then: how long do we have to make these guard rings?

One way to answer this question is to build a prototype and test it by replacing the beam with a current flowing through a wire (see e.g. Baron and Vogel[1]). The wire, however, is a constant-potential surface while, for the beam, the potential along its length depends on the charge of the beam and the cross-section of the beam pipe. The consequence is, that the wire test underestimates the edge effect. Good results can be obtained by calibrating

the monitor with a cathode ray beam (Simanton[2]). For this, however, we need an expensive installation and, even then, it is still a cut and try procedure.

It would be useful to have some simple formulas for calculating the edge effect but, at first sight, it seems impossible to do this in a general way, due to the large number of possible configurations. In practice, however, the magnitude of the discontinuity is much more important than the exact configuration at the transition or the shape of the cross-sections at both sides. We will later see how we can replace circular or elliptical cross-sections by "equivalent" rectangular ones and then, most transitions more or less resemble the junction between beam pipes of different cross-section as shown on fig. 4;

We usually do not want to correct the measurements for the edge effect but, rather we want to construct the monitor in such a way that the errors can be neglected. In that case, a knowledge of the perturbations to, let's say $\pm 20\%$, is largely sufficient. This explains why a rather crude approximation can still give useful results. Our first step will now be, to compute the field in the vicinity of the junction of fig. 4 , for a beam, uniform in intensity along its length.

2; FIELD NEAR THE JUNCTION

We will compute the field in the vicinity of the junction between two rectangular beam pipes with different dimensions (fig. 4). We suppose the beam is thin, goes through (x_o, y_o), and has a uniform line charge of 1 Coulomb per meter. We suppose further that the pipe on the right has no dimension larger than the pipe on the left.

The field, far from the junction, can be calculated with the help of conformal mapping (see e.g. Kober[3]). We obtain $\varphi_{REFP}(x,y)$ for $z \gg 0$ and $\varphi_{REFN}(x,y)$ for $z \ll 0$. The electrostatic potential, φ , near the

junction, is then :

$$\varphi(z \geq 0) = \varphi_{REFP}(x,y) + \varphi_{PERTP}(x,y,z) \quad (1)$$

$$\varphi(z \leq 0) = \varphi_{REFN}(x,y) + \varphi_{PERTN}(x,y,z) \quad (2)$$

φ_{REF} is the field that would exist , in each pipe, in the absence of the junction. φ_{PERT} is the perturbation, due to the junction. φ and φ_{REF} are solutions of the Poisson equation and they are zero at the walls of both pipes. Consequently, we find that φ_{PERTP} and φ_{PERTN} are also zero at the walls and they are solutions of the Laplace equation, each in its domain. It follows, that the perturbation field is completely defined by the potential in the plane z=0 . Because of the continuity of φ at z=0 , we have :

$$\varphi_{REFP}(x,y) + \varphi_{PERTP}(x,y,0) = \varphi_{REFN}(x,y) + \varphi_{PERTN}(x,y,0) \quad (3)$$

$$\varphi'_{PERTP}(x,y,0) = \varphi'_{PERTN}(x,y,0) \quad (4)$$

All this for $|x| < a$ and $|y| < b$ and with $\varphi' = \partial\varphi/\partial z$. We define now the potential

$$V_{DIF}(x,y) = \varphi_{REFN}(x,y) - \varphi_{REFP}(x,y) \quad (5)$$

The perturbation field, at z=0 , can then be written in function of the known V_{DIF} and an unknown potential V_o :

$$\varphi_{PERTP}(x,y,0) = V_o(x,y) \quad (6)$$

$$\varphi_{PERTN}(x,y,0) = V_o(x,y) - V_{DIF}(x,y) \qquad |x| < a \text{ and } |y| < b \quad (7)$$

$$\varphi_{PERTN}(x,y,0) = -\varphi_{REFN}(x,y) \qquad |x| \geq a \text{ or } |y| \geq b \quad (8)$$

We will compute successive approximations for V_o , beginning with :

$$V_o(x,y) = V_{REFP}(x,y)/2 \quad (9)$$

With this value of V_o , we can express the perturbation field, at each side of the junction, in the form of a double Fourier expansion. For the positive side ($z \geq 0$), we find :

$$\varphi_{PERTP}(x,y,z) = \sum_{k=1}^{\infty}\sum_{m=1}^{\infty} A_{km} \sin\left[\frac{k\pi(x+a)}{2a}\right].\sin\left[\frac{m\pi(y+b)}{2b}\right].e^{-\alpha_{km}z} \qquad (10)$$

$$\text{with} \quad \alpha_{km} = \sqrt{\left(\frac{k\pi}{2a}\right)^2 + \left(\frac{m\pi}{2b}\right)^2} \quad \text{and} \qquad (11)$$

$$A_{km} = \frac{1}{a.b}\int_{-a}^{a}\int_{-b}^{b} V_o(x,y).\sin\left[\frac{k\pi(x+a)}{2a}\right].\sin\left[\frac{m\pi(y+b)}{2b}\right].dx.dy \qquad (12)$$

By differentiating eq. (10) according to z, we find the z-gradient of the field. For z=0 , we have :

$$\varphi'_{PERTP}(x,y,0) = -\sum_{k=1}^{\infty}\sum_{m=1}^{\infty} \alpha_{km}.A_{km}.\sin\left[\frac{k\pi(x+a)}{2a}\right].\sin\left[\frac{m\pi(y+b)}{2b}\right] \qquad (13)$$

The gradient on the negative side can be found by exchanging a^*, b^*, A^*_{km} and $(V_o - V_{DIF})$ for a, b, A_{km} and V_o. In general, φ'_{PERTP} will not be equal to φ'_{PERTN}, as required by eq.(4). We obtain a better approximation for φ'_{PERTP} with:

$$\bar{\varphi}'_{PERTP} = \frac{1}{2}\left(\varphi'_{PERTP} + \varphi'_{PERTN}\right) \qquad (14)$$

Now, we can find a better approximation for A_{km}, through inversion of (13) :

$$\bar{A}_{km} = -\frac{1}{a.b.\alpha_{km}}\int_{-a}^{a}\int_{-b}^{b}\bar{\varphi}'_{PERTP}(x,y,0).\sin\left[\frac{k\pi(x+a)}{2a}\right].\sin\left[\frac{m\pi(y+b)}{2b}\right].dx.dy \qquad (15)$$

and we find a better approximation for V_o, by putting the new values of A in eq.(10), for z=0 :

$$\bar{V}_o(x,y) = \sum_{k=1}^{\infty}\sum_{m=1}^{\infty}\bar{A}_{km}.\sin\left[\frac{k\pi(x+a)}{2a}\right].\sin\left[\frac{m\pi(y+b)}{2b}\right] \qquad (16)$$

With this improved value of V_o, we start a new iteration and so on, until the required precision is attained. That is, when in every point in the plane z=0 :

$$\left|\varphi'_{PERTP} - \varphi'_{PERTN}\right| < \epsilon\left|\varphi'_{PERTP}\right| \qquad (17)$$

with ϵ a sufficiently small value.

The calculation of the potentials in the cross-section was done on a grid of maximum 80x40 points. The smallest dimension was usually taken to be 20 points, sometimes 10 if some other dimension was too large. For $\epsilon = 0.01$, we need 3 to 4 iterations. For calculations on the full grid of 80x40 points, this takes about 4 seconds on a CDC7600 computer. As a result, we obtain the matrices A and A^* .

3. CHARGE ON THE WALL

Of special interest, for beam monitoring, is the charge, induced on the wall by the beam. By differentiating eq.(10), we obtain the charge induced by the perturbation field. For instance :

$$\sigma_{PERTP}(-a,y,z) = -\epsilon_o\left[\frac{\partial \varphi_{PERTP}}{\partial x}\right]_{x=-a} = -\sum_{k=1}^{\infty}\sum_{m=1}^{\infty} \frac{k\pi\epsilon_o A_{km}}{2a} \cdot \sin\left[\frac{m\pi(y+b)}{2b}\right] \cdot e^{-\alpha_{km} z} \quad (18)$$

and 7 similar formulas for the other sides. We can do the same for the reference field :

$$\sigma_{REFP}(-a,y) = -\epsilon_o\left[\frac{\partial \varphi_{REFP}}{\partial x}\right]_{x=-a} \quad (19)$$

Finally, we can integrate σ over the width of the wall. We find the line charges :

$$q_{LPERTP}(x=-a,z) = \int_{-b}^{b} \sigma_{PERTP}(-a,y,z)\,dy = -2\sum_{k=1}^{\infty}\sum_{m=1,3,5\ldots}^{\infty} \frac{bk}{am} A_{km} \cdot e^{-\alpha_{km} z} \quad (20)$$

$$q_{LREFP}(x=-a) = \int_{-b}^{b} \sigma_{REFP}(-a,y)\,dy \quad (21)$$

4. SOME RESULTS

To get a feeling for how far the perturbations reach, a few configurations are shown on fig. 5. All dimensions are in meter. The beam has a uniform charge of 1C/m . XO, YO indicates the position of the beam. ALARGE, BLARGE, ASMALL, BSMALL, are half the dimensions of the large and small beam pipes. The sides are numbered as indicated. For each side, we calculate q_{LREF} and :

$$q_{LREL} = \frac{q_{LPERT} + q_{LREF}}{q_{LREF}} \qquad (22)$$

This dimensionless ratio is plotted in function of the distance from the junction: z= LxSTEPL . In example A, we plot q_{LREL} from 0 to 2. In the other examples, only the more interesting region between 0.8 and 1.2 is plotted.

5. INTENSITY MODULATED BEAM

We will now see what happens when the beam is not a uniform line charge. A diffuse beam can be calculated as if it was a line charge, going through the charge center. This gives good results when the diameter of the diffuse beam is smaller than the distance of the charge center to the nearest wall.

A beam, varying in intensity along its length, can be expanded in its Fourier components, with D_λ the amplitude of the component q_{LB}, with wavelength λ :

$$q_{LB} = D_\lambda \cdot \cos\left[\frac{2\pi}{\lambda}(V.t + z_\lambda - z)\right] \qquad (23)$$

q_{LB} is the line charge of the Fourier component, V is the speed of the particles in the beam (with $\omega = 2\pi V/\lambda$ the angular frequency) and $2\pi z_\lambda/\lambda$ is a phase angle.

We limit ourselves to the case where $\gamma\lambda$ is large with respect to 2a or 2b (γ is the ratio of the mass of the

particles to their rest mass). In that case the potential, far from the junction, is given by the field of a uniform beam, modulated with q_{LB} (Cupérus[4]). V_{DIF} at the junction is then equal to V_{DIF} for the uniform beam, modulated with $q_{LB}(z=0)$. This V_{DIF} excites TM waves on both sides of the junction. The relation between E_x, E_y and E_z for z=0 is :

$$E_x = - \frac{\alpha'_{km}}{\alpha^2_{km}} \cdot \frac{\partial E_z}{\partial x} \tag{24}$$

$$E_y = - \frac{\alpha'_{km}}{\alpha^2_{km}} \cdot \frac{\partial E_z}{\partial y} \tag{25}$$

$$\alpha'_{km} = \sqrt{\left(\frac{k\pi}{2a}\right)^2 + \left(\frac{m\pi}{2b}\right)^2 - \left(\frac{\omega}{c}\right)^2} \tag{26}$$

with c the speed of light in vacuum.

Beam monitoring is not possible at frequencies where the waves can propagate in the beam pipe. We find, for the critical frequency ω_c (and $a \gg b$) :

$$\omega_c = \pi c / 2a \tag{27}$$

The TE_{10} mode is not directly excited at the junction. For the TM_{11} mode, we find, for $\omega = 0.7\omega_c$ and a=b :

$$\alpha'_{11} = \sqrt{\left(\frac{\pi}{2a}\right)^2 + \left(\frac{\pi}{2b}\right)^2 - \frac{1}{2}\left(\frac{\pi}{2a}\right)^2} = 0.87\,\alpha_{11} \tag{28}$$

Even in this unfavorable case, α'_{11} is not very different from α_{11} . The correspondence is better for higher modes and lower frequencies. We see that, at z=0, the relation between transversal and longitudinal components of E is allmost independent of frequency (below $0.7\omega_c$) and the solution for the perturbation field at z=0 is valid at all useful frequencies. For $z \neq 0$, we use (18) and (20), where we substitute α'_{km} for α_{km} . So, even at $z \neq 0$, we can use the solution for the uniform beam as a fair approximation. The perturbation field, however, is modulated with $q_{LB}(z=0)$ while the reference field is modulated with $q_{LB}(z)$.

What is said above is, of course, also valid for the large beam pipe, provided we substitute a^* and b^* for a and b. In the remainder of this paper, we will slightly modify the notations: the monitor is now on the side $z > 0$, with beam pipe dimensions $2a$ and $2b$. The beam pipe dimensions on the other side are $2w$ and $2h$. w and h can now be smaller or larger than a and b. All field calculations will be made for $z > 0$ only.

6. CIRCULAR AND ELLIPTICAL CROSS SECTIONS

For the circular cross-section, we can repeat all the calculations. There are difficulties because of the concentration of grid points in the center. Also, the computations for Bessel functions are much longer than for trigonometric functions. These difficulties can be overcome but, if we are content with good approximations, it is easier to replace the circular or elliptical cross-sections by "equivalent" rectangular cross-sections and to calculate everything as if the beam pipes and the monitor were indeed rectangular.

The first two TM modes are the most important and, for the square cross-section with sides 2a, they decay with $A_{11}\exp(-\pi z/\sqrt{2}a)$ and $A_{12}\exp(-\pi\sqrt{5}z/2a)$. For the circular cross-section, with radius 2R, this corresponds to $A_{01}\exp(-2.40z/R)$ and $A_{11}\exp(-3.83z/R)$. The exponents in the corresponding modes are equal when $a=0.925R$ and $a=0.916R$. We define the "equivalent" square cross-section with:

$$a = 0.92\,R \tag{29}$$

We can extend this result and replace the ellipse by an "equivalent" rectangle with sides 0.92 times the axes of the ellipse.

7. SUM AND DIFFERENCE CHARGES

For practical applications, we are interested in the sum and difference of the perturbation charges on opposite sides of the beam monitor. For the vertical walls, we have:

$$q_{L\Sigma X}(z) = q_{LPERT}(a,z) + q_{LPERT}(-a,z) \tag{30}$$

$$q_{L\Delta X}(z) = q_{LPERT}(a,z) - q_{LPERT}(-a,z) \tag{31}$$

and, with eq. (20) and similar formulas:

$$q_{L\Sigma X}(z) = -4\frac{\ell}{a}\epsilon_0\left\{A_{11}e^{-\alpha_{11}z} + \frac{1}{3}A_{13}e^{-\alpha_{13}z} + 3A_{31}e^{-\alpha_{31}z}\ldots\right\} \tag{32}$$

$$q_{L\Delta X}(z) = 4\frac{\ell}{a}\epsilon_0\left\{2A_{21}e^{-\alpha_{21}z} + 4A_{41}e^{-\alpha_{41}z}\ldots\right\} \tag{33}$$

The total sum and difference charge that falls on the vertical walls for $z \geqslant g$ is :

$$q_{\Sigma X}(g) = \int_g^\infty q_{L\Sigma X}(z)\,dz = -4\frac{\ell}{a}\epsilon_0\left\{\frac{A_{11}}{\alpha_{11}}e^{-\alpha_{11}g} + \frac{A_{13}}{3\alpha_{13}}e^{-\alpha_{13}g} + \frac{3A_{31}}{\alpha_{31}}e^{-\alpha_{31}g}\ldots\right\} \tag{34}$$

$$q_{\Delta X}(g) = \int_g^\infty q_{L\Delta X}(z)\,dz = \frac{4\ell}{a}\epsilon_0\left\{\frac{2A_{21}}{\alpha_{21}}\cdot e^{-\alpha_{21}g} + \frac{4A_{41}}{\alpha_{41}}e^{-\alpha_{41}g}\ldots\right\} \tag{35}$$

Close to the junction, the higher order terms are important and the perturbation is very large. For $g > 1/\alpha_{11}$, however, we can neglect the higher order terms. For a beam with uniform charge D (C/m), we find :

$$q_{\Sigma X}(g) = \frac{\ell}{a}\cdot\frac{D\cdot F_{11}}{\alpha_{11}}\cdot e^{-\alpha_{11}g} \tag{36}$$

$$q_{\Delta X}(g) = \frac{\ell}{a}\cdot\frac{D\cdot F_{21}}{\alpha_{21}}\cdot e^{-\alpha_{21}g} \tag{37}$$

and, for the horizontal walls :

$$q_{\Sigma Y}(g) = \frac{a}{\ell}\cdot\frac{D\cdot F_{11}}{\alpha_{11}}\cdot e^{-\alpha_{11}g} \tag{38}$$

$$q_{\Delta Y}(g) = \frac{a}{\ell}\cdot\frac{D\cdot F_{12}}{\alpha_{12}}\cdot e^{-\alpha_{12}g} \tag{39}$$

F_{11} , F_{12} and F_{21} are dimensionless and in value equal to:

$$F_{11} = -4\epsilon_0 A_{11} \quad ; \quad F_{12} = 8\epsilon_0 A_{12} \quad ; \quad F_{21} = 8\epsilon_0 A_{21} \tag{40}$$

We will tabulate F for two common transitions, the "conformal" transition and the "square to rectangle" transition.

8. CONFORMAL TRANSITION

By this, we mean a transition such that $w/a = h/b = \rho$. F_{11} was calculated for a centered beam and several values of ρ . Table 1 gives a few results. A first conclusion is that F_{11} does not change much with the ratio a/b.

F_{11} was also calculated for other beam positions. We found that F_{11} changes little ($\pm$10%) with the position of the beam, when $\rho<1$. For $\rho>1$, F_{11} varies by about $\pm$20% when the beam moves within a reference ellipse (defined as the ellipse with axes 0.8 times the dimensions of the smallest beam pipe), with a maximum when the beam moves to the middle of the largest side and a minimum towards the corners.

F_{12} and F_{21} were calculated for several values of ρ , x_o and y_o . When the beam moves over the x or y axis, the results can be expressed by the empirical formulas:

$$F_{12} = \frac{y_o}{\sqrt{a.b}} F(\rho) \qquad F_{21} = \frac{x_o}{\sqrt{a.b}} F(\rho) \tag{41}$$

with $F(\rho)$ given by table 2. For a beam within the reference ellipse, these formulas, together with the table, give values for F_{12} and F_{21} , accurate within $\pm$15% .

9. TRANSITION FROM RECTANGLE TO SQUARE

We now consider the transition between a square beam monitor, with side2a, and a rectangular beam pipe

with height 2h and width 2w=2a (see e.g. fig. 5D). The perturbation field in the monitor is given by :

$$F_{11} = 0.36 \quad \text{for} \quad h = 0.50a \tag{42}$$

$$F_{11} = 0.19 \quad \text{for} \quad h = 0.66a \tag{43}$$

F_{11} goes to zero when $|x_o|$ goes to a and $|F_{11}|$ is about 25% higher than in the center, for $|x_o| = 0$ and $|y_o| = 0.8h$.

$|F_{21}|$ is small. F_{12} is approximatively given by the empirical formulas:

$$F_{12} = 0.55 y_o/h \quad \text{for } h = 0.50a \tag{44}$$

$$F_{12} = 0.42 y_o/h \quad \text{for } h = 0.66a \tag{45}$$

10. EDGE EFFECT FOR THE ELECTROSTATIC PICKUP

We use the "equivalent" rectangular cross-sections (as defined in §6) and suppose the transitions to be conformal with ρ_1 on the left and ρ_2 on the right. ρ is smaller than 1 for the example of fig. 1 and larger than 1 for fig. 2.

To reduce the effect of the transitions, we use guard rings with lengths g_1 and g_2 . We suppose the electrodes grounded and calculate the total charge that would fall on the electrodes E_1 and E_2 in the absence of the junctions. For a uniform beam, with charge D Coulomb/m, we find :

$$q_{E1} + q_{E2} = - D.L \tag{46}$$

with L the length of the pickup electrodes. With the junctions present, the real charges on the electrodes are $q_{E1} + q_{P1}$ and $q_{E2} + q_{P2}$. q_{P1} and q_{P2} are the perturbation charges, due to the junctions. For intensity measurements, we are interested only in the sum of the charges on both electrodes and the relative error, η, due to the junctions is :

$$\eta \cong \frac{q_{P1}+q_{P2}}{q_{E1}+q_{E2}} \cong -\frac{1}{D.L}\left[q_{\Sigma X}(g_1)+q_{\Sigma Y}(g_1)+q_{\Sigma X}(g_2)+q_{\Sigma Y}(g_2)\right] \quad (47)$$

and, with eq. (36) and (38) :

$$\eta \cong -\frac{2\sqrt{a^2+b^2}}{\pi L}\left[F_{II}(\rho_1).e^{-\frac{\pi}{2}\sqrt{\frac{1}{a^2}+\frac{1}{b^2}}\,g_1} + F_{II}(\rho_2)\,e^{-\frac{\pi}{2}\sqrt{\frac{1}{a^2}+\frac{1}{b^2}}\,g_2}\right] \quad (48)$$

This formula is accurate only when g_1 and g_2 are large enough, so that we can neglect the higher terms. As a practical rule, we can say that the exponents of e, in the formula above, must be larger than 1, in absolute value.

As an example, we take 2a=2b=12cm , L=10cm , $\rho_1=\rho_2=2$. From table 1, we take F_{II}=-0.145 and (48) is then, for a centered beam :

$$\eta = 0.078\left(e^{-g_1/0.027} + e^{-g_2/0.027}\right)$$

For $g_1=g_2=3$cm , η is about 5%. The variation in the error is from 4 to 6% when the beam moves within the reference ellipse.

We now want to study the position, measured with:

$$P_X(x_o) = \frac{(q_{E1}+q_{P1})-(q_{E2}+q_{P2})}{(q_{E1}+q_{P1})+(q_{E2}+q_{P2})}\,a \quad (49)$$

When the perturbation charges are zero, we have, with the linear electrodes of figs. 1 and 2: $P_X(x_o)=x_o$ (Sherwood[5]). We will now study the deviations from this linear response, due to the transitions.

10.1 Center Displacement

For the calculation of the center displacement, we can consider the right and left junctions separately. The total displacement is then the algebraic sum of the two displacements. For a configuration, symmetrical with respect to the center of the PU, both displacements neutralise each other and $P_X(0)=0$.

The configuration is asymmetrical, when $\rho_1 \neq \rho_2$ or $g_1 \neq g_2$ or when the electrode configuration itself is not symmetrical (as can occur, for instance, when the electrodes for horizontal and vertical position measurement are brought together in one monitor with 4 electrodes). For a centered beam we find, for the center displacement Δx_o , due to the left transition :

$$\Delta x_o \cong \frac{q_{E1} - q_{E2} + q_{\Sigma Y}(g_1)}{q_{E1} + q_{E2} + q_{\Sigma X}(g_1) + q_{\Sigma Y}(g_1)} \cong - \frac{q_{\Sigma Y}(g_1)}{D.L}\, a \qquad (50)$$

We suppose here, that $q_{\Sigma Y}$ falls entirely on electrode E_1. This results in a slight overestimation of the edge effect. With (38), we find:

$$\Delta x_o \cong - \frac{a^2}{b} \cdot \frac{F_{11}}{\alpha_{11} L} \cdot e^{-\alpha_{11} g_1} \qquad (51)$$

For example, with 2a=20cm, 2b=14cm, L=14cm and ρ_1=1.5, we find from table 1 (interpolating between the values for a=b and a=2b) : F_{11}=-0.108 and :

$$\Delta x_o \cong 0.0040 \cdot e^{-g_1/0.037}$$

If we want Δx_o to be smaller than 1mm, g_1 must be larger than 50mm.

10.2 Errors in the Scale Factor

We now suppose the configurations of figs. 1 and 2 to be symmetrical, with $g_1=g_2=g$, $\rho_1=\rho_2=\rho$ and, consequently, $\Delta x_o=0$. Eq: (49) is then :

$$P_x(x_o) = \frac{q_{E1} - q_{E2} + 2q_{\Delta X}(g)}{q_{E1} + q_{E2} + 2q_{\Sigma X}(g) + 2q_{\Sigma Y}(g)}\, a \qquad (52)$$

and the scale factor is

$$P'_x(x_o) = d\,P_x(x_o)/dx_o = 1 + \zeta \qquad (53)$$

with

$$\zeta \cong \frac{2}{D.L}\left[a\,\frac{dq_{\Delta x}(g)}{dx_o} - q_{\Sigma X}(g) - q_{\Sigma Y}(g)\right] \qquad (54)$$

and, with eq. (36) to (39) and (41):

$$\zeta \cong \frac{4}{\pi L}\left\{\sqrt{\frac{b}{a}} \cdot \frac{F(\rho).e^{-\alpha_{21} g}}{\sqrt{4/a^2 + 1/b^2}} - \sqrt{a^2+b^2}\cdot F_{11}\cdot e^{-\alpha_{11} g}\right\} \qquad (55)$$

For g=0, the second term is already larger than the first, in absolute value. Moreover, the first decays faster with g. For $g\alpha_{11}>1$, we can write :

$$\zeta = -\frac{4\sqrt{a^2+b^2}}{\pi L}\cdot F_{11}\cdot e^{-\alpha_{11} g} \qquad (56)$$

For example, with 2a=20cm, 2b=14cm, L=14cm and ρ =0.9 , we find from table 1 (with interpolation): F =0.062 and:

$$\zeta = -0.069\, e^{-g/0.037}$$

If we want ζ to be smaller than 2% , g must be larger than 46mm.

11. WALL CURRENTS

The Fourier component, with wavelength λ, of the beam current is :

$$i_B = q_{LB}.V = D_\lambda.V.\cos\left[\frac{2\pi}{\lambda}(V.t + z_\lambda - z)\right] \qquad (57)$$

This Fourier component induces, near the junction (at z=0), a time-dependent perturbation charge q_{LPERT} . This causes an alternating current in the wall, approximatively in the z-direction. To simplify the calculations, we will suppose that the current does not cross the corners of the beam pipe.

We can again calculate the sum and difference of the perturbation currents on opposite walls, for z=g :

$$i_{\Sigma X}(g) = \frac{d}{dt}\left\{q_{\Sigma X}(g).\cos\left[\frac{2\pi}{\lambda}(V.t + z_\lambda)\right]\right\} \qquad (58)$$

$$i_{\Delta X}(g) = \frac{d}{dt}\left\{q_{\Delta X}(g).\cos\left[\frac{2\pi}{\lambda}(V.t + z_\lambda)\right]\right\} \qquad (59)$$

And, with $q_{\Sigma X}$ and $q_{\Delta X}$ given by (36) and (37):

$$i_{\Sigma X}(g) = -\frac{2\pi}{\lambda} \cdot I_B \cdot \frac{b}{a} \cdot \frac{F_{11}}{\alpha_{11}} \cdot e^{-\alpha_{11} g} \cdot \sin\left[\frac{2\pi}{\lambda}(V.t + z_\lambda)\right] \qquad (60)$$

$$i_{\Delta X}(g) = -\frac{2\pi}{\lambda} \cdot I_B \cdot \frac{b}{a} \cdot \frac{F_{21}}{\alpha_{21}} \cdot e^{-\alpha_{21} g} \cdot \sin\left[\frac{2\pi}{\lambda}(V.t + z_\lambda)\right] \qquad (61)$$

with $I_B = D_\lambda . V$ the amplitude of the Fourier-component of the beam current. For the horizontal walls, we find:

$$i_{\Sigma Y}(g) = -\frac{2\pi}{\lambda} \cdot I_B \cdot \frac{a}{b} \cdot \frac{F_{11}}{\alpha_{11}} \cdot e^{-\alpha_{11} g} \cdot \sin\left[\frac{2\pi}{\lambda}(V.t + z_\lambda)\right] \qquad (62)$$

$$i_{\Delta Y}(g) = -\frac{2\pi}{\lambda} \cdot I_B \cdot \frac{a}{b} \cdot \frac{F_{12}}{\alpha_{12}} \cdot e^{-\alpha_{12} g} \cdot \sin\left[\frac{2\pi}{\lambda}(V.t + z_\lambda)\right] \qquad (63)$$

12. EDGE EFFECT FOR THE WALL CURRENT MONITOR

A wall current monitor (Avery et al.[6]) is usually circular in cross-section. A junction with elliptical beam pipes causes perturbation fields. As discussed before, we can replace the circular and elliptical cross-sections by "equivalent" rectangular cross-sections and then, we obtain the configuration of fig. 3. We suppose the shunt over the gap to be of low impedance. The total current, flowing over the shunt, is then $-\bar{I}_B + \bar{I}_P$ with $\bar{I}_B$ the Fouriercomponent, with wavelength λ , of the beam and $\bar{I}_P$ the complex amplitude of the perturbation current, due to the junctions. With $g_1 = g_2 = g$ and eq. (60) and (62), we find (considering that the perturbation fields due to the left and right junctions are out of phase by $4\pi g/\lambda$):

$$\frac{I_P}{I_B} = 4\frac{\sqrt{a^2+b^2}}{\lambda} \cdot F_{11} \cdot e^{-\frac{\pi}{2}\sqrt{\frac{1}{a^2}+\frac{1}{b^2}}\, g} \cdot 2\sin\left(\frac{2\pi g}{\lambda}\right) \qquad (64)$$

And the phase difference between $\bar{I}_B$ and $\bar{I}_P$ is 90°.

For example, with a=b=w=8cm, h=4cm, f=200MHz and V=c, we find: λ =1.5m, F_{11} =0.36 (with eq.42) and

$$\frac{I_P(g)}{I_B} = 0.108 \cdot e^{-g/0.036} \cdot 2 \sin(g/0.24)$$

With g=8cm : I_P/I_B=0.008. We see that, even for 200MHz, the error due to the transitions is small, at least for the common symmetrical configuration.

For position measurements, the gap is divided in 4 sectors which we make correspond to the 4 walls of the beam pipe. The discussion is analogeous to that for the ESPU and will not be repeated here, because the errors are very small for the symmetric configuration.

REFERENCES

1. A.I.Baron and U.Vogel, Rev.Sci.Instr., Vol. 41, Nr. 12 (1970) 1832.

2. J.R.Simanton, IEEE Trans.Nucl.Sci.,NS-16, Nr.3 (1969) 932.

3. H.Kober, Dictionary of Conformal Representations, Dover 1952, p.170.

4. J.H.Cupérus, to be published in Nuclear Instuments and Methods.

5. A.J.Sherwood, IEEE Trans.Nucl.Sci. NS-12 (1965) 925.

6. R.T.Avery, A.Faltens and E.C.Hartwig, IEEE Trans.Nucl. Sci. NS-18 (1971) 920.

TABLE 1

ρ	$F_{\parallel}$ for a=b	$F_{\parallel}$ for a=2b or b=2a
0.8	+0.151	+0.122
0.9	+0.068	+0.055
1.1	-0.037	-0.032
1.2	-0.063	-0.056
1.5	-0.112	-0.104
2	-0.145	-0.141
3	-0.182	-0.180
4	-0.199	-0.200

TABLE 2

ρ	$F(\rho)$
0.8	+0.312
0.9	+0.127
1.1	-0.050
1.2	-0.076
1.5	-0.116
2	-0.132
3	-0.140
4	-0.144

FIGURE CAPTIONS

fig. 1 : Electrostatic position monitor, larger than the beam pipe, for protection against stray particles.

fig. 2 : Electrostatic position monitor, mounted in a large vacuum chamber.

fig. 3 : Wall current monitor of circular cross section, joined to beam pipes with elliptical or rectangular cross sections.

fig. 4 : Junction between rectangular beam pipes with different dimensions.

fig. 5 : Charge on the wall of the beam pipe, normalised to the charge far from the junction. A and B are half the dimensions of the pipes and XO, YO is the beam position. z=LxSTEPL is the distance from the junction.

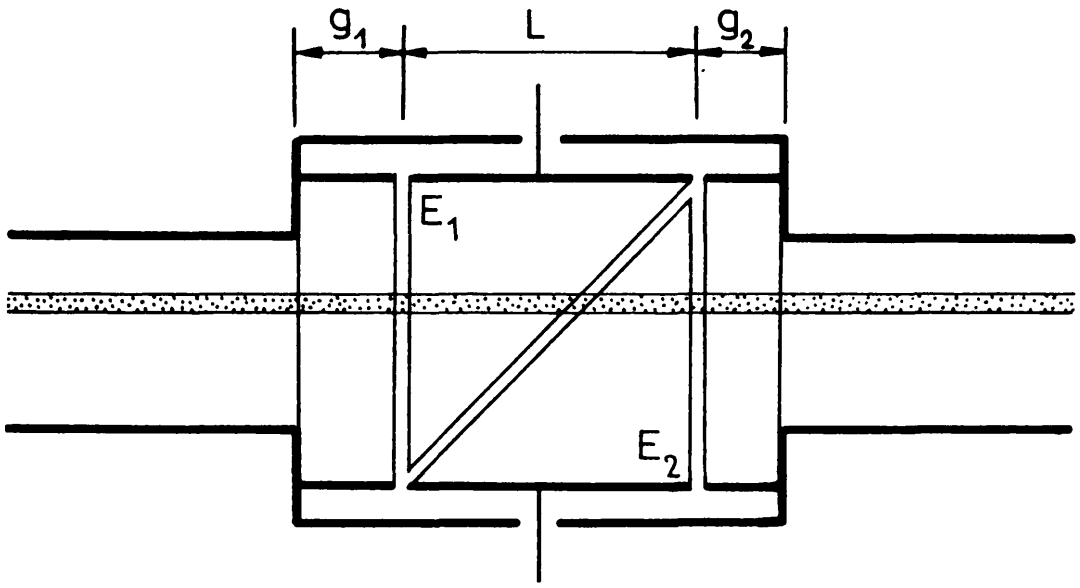

FIG.1

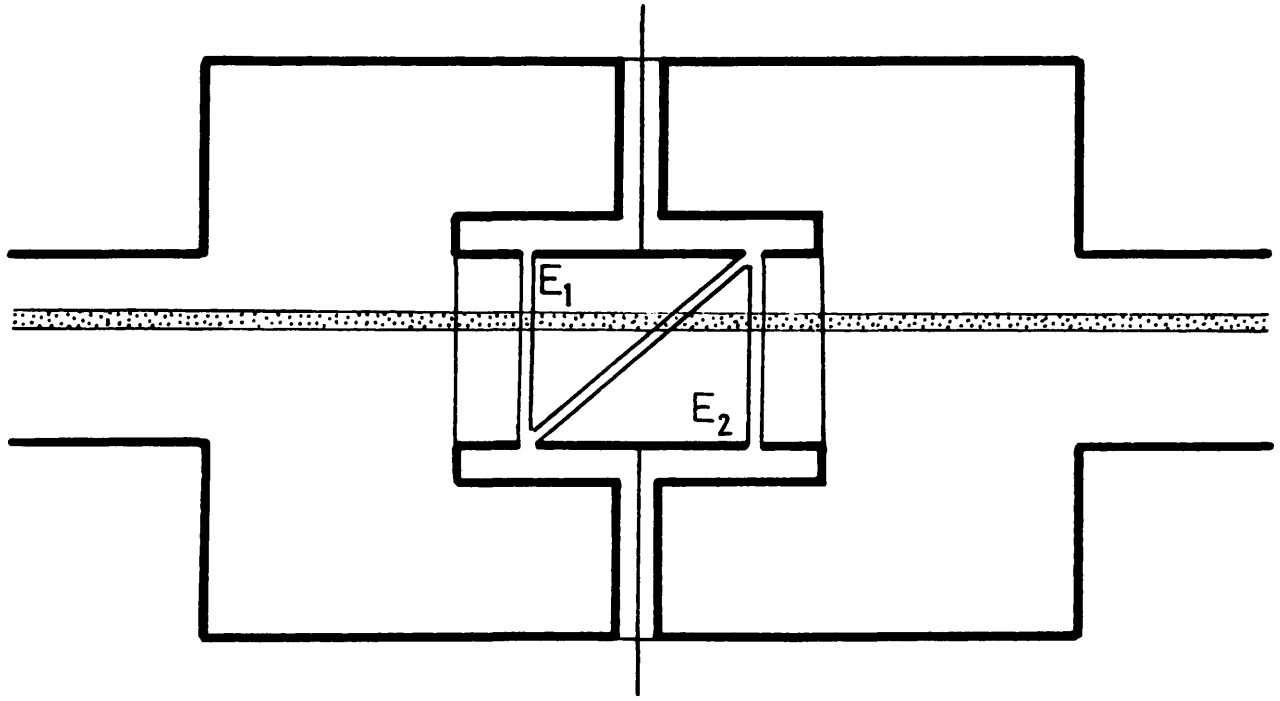

FIG. 2

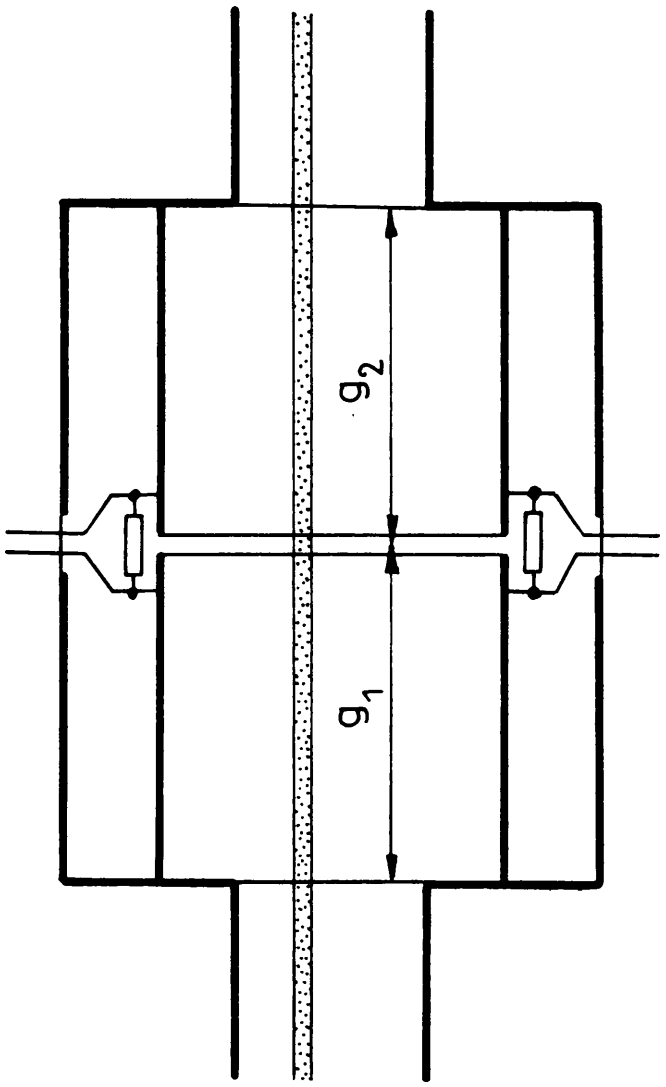

FIG. 3

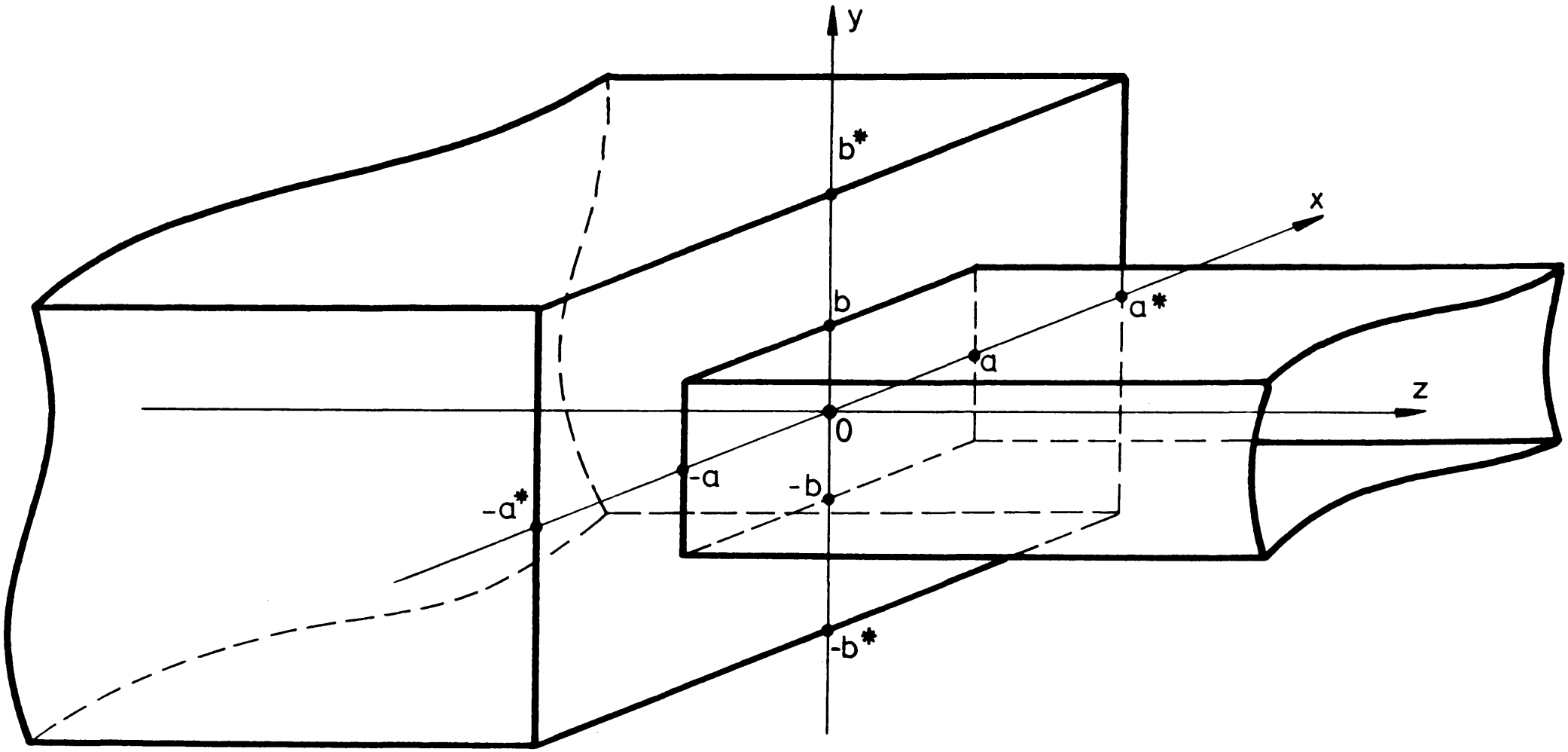

FIG.4

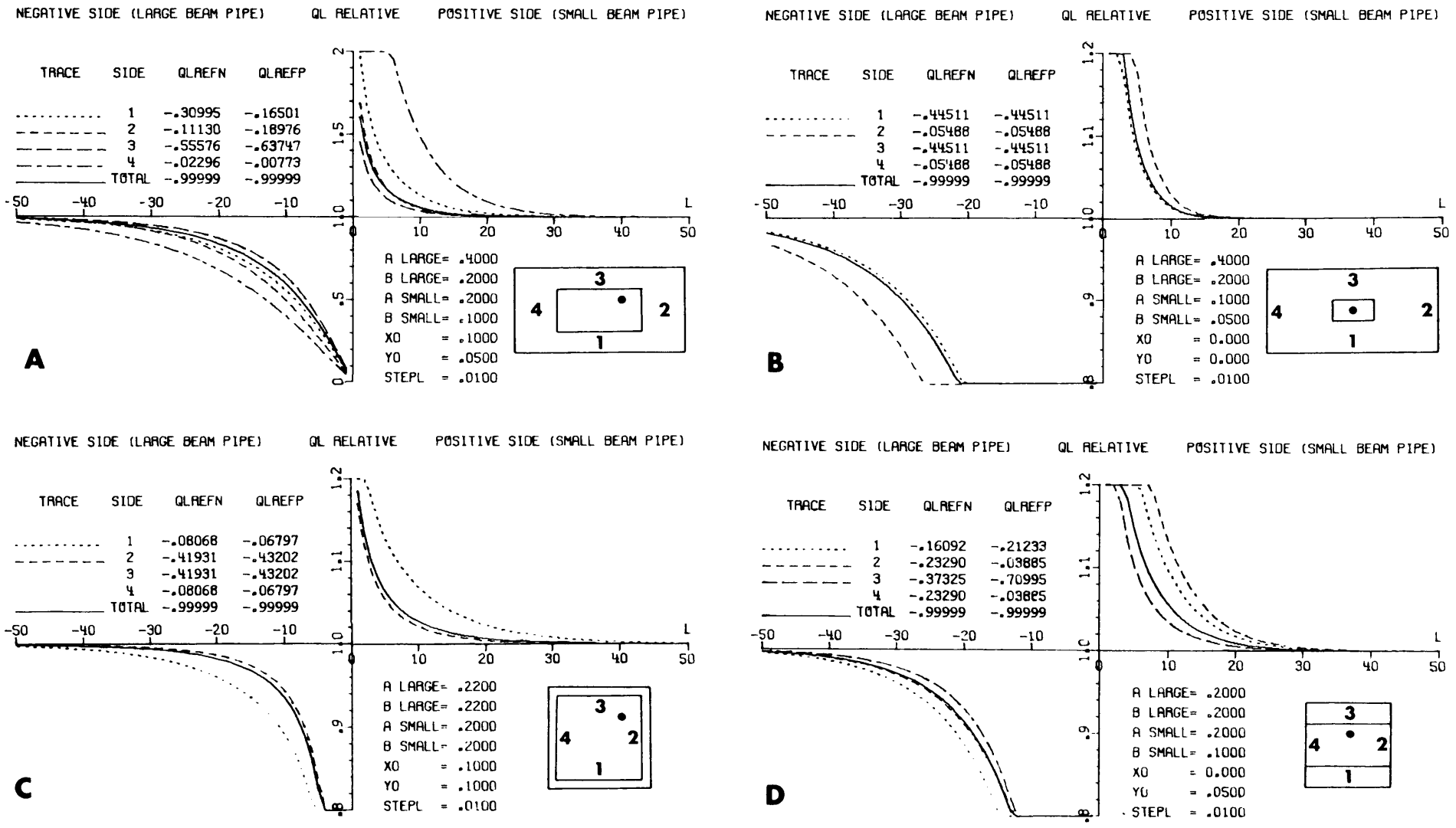
NEGATIVE SIDE (LARGE BEAM PIPE) QL RELATIVE POSITIVE SIDE (SMALL BEAM PIPE)
TRACE SIDE QLREFN QLREFP
1 -.30995 -.16501
2 -.11130 -.18976
3 -.55576 -.63747
4 -.02296 -.00773
TOTAL -.99999 -.99999
A LARGE= .4000
B LARGE= .2000
A SMALL= .2000
B SMALL= .1000
XO = .1000
YO = .0500
STEPL = .0100
A
NEGATIVE SIDE (LARGE BEAM PIPE) QL RELATIVE POSITIVE SIDE (SMALL BEAM PIPE)
TRACE SIDE QLREFN QLREFP
1 -.44511 -.44511
2 -.05488 -.05488
3 -.44511 -.44511
4 -.05488 -.05488
TOTAL -.99999 -.99999
A LARGE= .4000
B LARGE= .2000
A SMALL= .1000
B SMALL= .0500
XO = 0.000
YO = 0.000
STEPL = .0100
B
NEGATIVE SIDE (LARGE BEAM PIPE) QL RELATIVE POSITIVE SIDE (SMALL BEAM PIPE)
TRACE SIDE QLREFN QLREFP
1 -.08068 -.06797
2 -.41931 -.43202
3 -.41931 -.43202
4 -.08068 -.06797
TOTAL -.99999 -.99999
A LARGE= .2200
B LARGE= .2200
A SMALL= .2000
B SMALL= .2000
XO = .1000
YO = .1000
STEPL = .0100
C
NEGATIVE SIDE (LARGE BEAM PIPE) QL RELATIVE POSITIVE SIDE (SMALL BEAM PIPE)
TRACE SIDE QLREFN QLREFP
1 -.16092 -.21233
2 -.23290 -.03885
3 -.37325 -.70995
4 -.23290 -.03885
TOTAL -.99999 -.99999
A LARGE= .2000
B LARGE= .2000
A SMALL= .2000
B SMALL= .1000
XO = 0.000
YO = .0500
STEPL = .0100
D

FIG. 5